Heliyon 5 (2019) e02227

Contents lists available at ScienceDirect

Heliyon

journal homepage: www.heliyon.com

Numerical evaluation of cooling performances of semiconductor using CuO/water nanofluids

P.C. Mukesh Kumar [a,*], C.M. Arun Kumar [b]

[a] Department of Mechanical Engineering, University College of Engineering, Dindigul, Tamilnadu, 624622, India
[b] Department of Electronics and Communication Engineering, University College of Engineering, Pattukottai, Tamilnadu, 614701, India

ARTICLE INFO

Keywords:
Nanotechnology
Electronic cooling
ANSYS-CFD
Channel heat sink
Reliability
Nanofluids
Computational materials science
Computer-aided engineering
Nanomaterials
Very-large-scale integration

ABSTRACT

Now a days Very-Large-Scale Integrated (VLSI) circuits are facing critical issues to satisfy the cooling demand because of shrinking the semiconductors. In this numerical work, the surface temperature of the chip, heat transfer rate, thermal resistance, power consumption and reliability are studied by using CuO/water nanofluids as coolant and compared the nanofluids results with the results of water. The CuO/water nanofluids at 0.25%, 0.5%, and 0.75% volume concentration are used for this investigation. The modelling, meshing and simulation are carried out by CATIAv5 and ANSYS Fluent v12 CFX software package. It is observed that the heat transfer rates of semiconductor using the coolant CuO/water nanofluid at 0.25%, 0.5%, and 0.75% volume concentrations are 25%, 43%, and 57% respectively higher than that of water. Found that the surface temperature of the semiconductor is lowered by 3%, 6%, and 8%, the thermal resistances decrease up to 6%, 10%, and 13%, and the Nusselt number increases by 25%, 43%, and 56%, when compared to water. It is also studied that the power consumption of the semiconductor reduces by 3%, 6%, and 8% at 0.25%, 0.5%, and 0.75% volume concentration respectively than water as coolant. It is also found that the failure rate of the semiconductor of using CuO/water nanofluids at 0.25%, 0.5%, and 0.75% volume concentration are 69%, 76%, and 84% respectively smaller than the water.

1. Introduction

The fast growth of electronic devices is the urgent need for compact modern cooling technology to provide better performance with reliable operations. The high power consumption and lesser life are the challenging issues of electronic components. Several methods of electronic cooling technology are being proposed by the researchers. Showing interest in electronics cooling is one among them. Many researchers have studied the effect of a different combination of nanofluids to improve the cooling performance in the electronic devices. Tuckerman [1] investigated the electronic cooling in integrated circuits. They suggested that enhanced heat dissipation by using microscopic channel heat sinks is due to the power density of 790 W/cm^2 heat flux.

Wei and Joshi [2] found that a reduction in thermal resistance is achieved by optimizing the channel configuration such as aspect ratio, fin thickness and a ratio of channel width to fin thickness. Many techniques are being used for electronic cooling, particularly by making the coolant as jet and bombarding on the device to be cooled and also doing continuous evaporation and condensation to absorb and reject the heat [3, 4]. Many researchers have developed such techniques by inserting fins to effectively dissipate heat [5, 6, 7]. In general, the traditional electronic cooling systems supply the coolant by using a circulating mechanical pump. But, these systems are of bulky mass, consume more power and they provide uncertain measurements. Jajja et al. [8]investigated the thermal management of higher heat generation in microprocessors with five different heat sinks and by varying fin spacing in the order of 0.2 mm, 0.5 mm, 1.0 mm, and 1.5 mm in a flat plate heat sink. They found that the base temperature and thermal resistance of the heat sinks are dropped by reducing the fin spacing and by increasing the volume flow rate of circulating coolant through the heat sink.

Toh et al. [9]numerically investigated the cooling behaviour of an electronic device. They investigated the laminar flow condition and used finite volume method for solving the heat transfer equation. It was found that the viscosity and friction losses are reduced by increasing the temperature at the given Reynolds number. Tiselj et al. [10] investigated the role of conduction heat transfer in a heat sink. They proposed that the coolant and surface wall shows a nonlinear response across heat transfer.

Xie et al. [11, 12] worked on the straight microchannel heat sink

* Corresponding author.
E-mail address: pcmukeshkumar1975@gmail.com (P.C. Mukesh Kumar).

https://doi.org/10.1016/j.heliyon.2019.e02227
Received 24 January 2019; Received in revised form 11 July 2019; Accepted 1 August 2019

using water as coolant and investigated the heat transfer behaviour. Cova et al. [13] studied the cooling effect of power converters which handles water as coolant in the heatsink. Conrad et al. [14] observed the performance of a heat sink with pin fin on the chip. They studied the thermal behaviour was studied when the heatsink structure has physical contact with the coolant. The higher cooling demand made the development of an alternate method to enhance the thermal conductivity of a fluid by suspending the nano-sized particles in the range of 1–100nm in the base fluids. Choi of USA suggested the unique heat transfer fluids which consist of added nanoparticles in the base fluids [15]. The works on nanofluids are intense now to prove the potential benefits of applicability [16, 17, 18].

Sajid et al. [19]studied the thermal conductivity of hybrid nanofluids by considering the factors like nanoparticles materials, adding the amount of more of nanoparticles, types of base fluid, size of nanoparticle, temperature, and addition of surfactant, pH level and sonicating time. They also reviewed the research work on thermal conductivity of hybrid nanofluids experimentally, numerically and the work using soft computing tools (Artificial Neural Networking) to assess the applicability of nanofluids as coolant. Ali et al. [20]critically reviewed the techniques for preparing nanofluids and their physical properties such as thermal conductivity and viscosity. They analysed and concluded the cost of preparing nanofluids, nanoparticles settlement, surface tension, the environmental and social impact of using nanofluids, erosion of heat transfer surfaces are the major issues in using nanofluids. Moreover, use of surfactant improves the stability of nanofluids when compared with nanofluids without surfactant.

Sajid et al. [21] reviewed the heat transfer applications of nanofluids and the effects of nanoparticles concentration, size, shape, and nanofluid flow rate on Nusselt number, heat transfer coefficient, thermal conductivity, thermal resistance, friction factor and pressure drop. They reviewed the application of nanofluids in radiators, circular tube heat exchangers, plate heat exchangers, shell and tube heat exchangers and heat sinks. They also reviewed the various theoretical correlations for experimental validation and suggested the pros and cons of applying nanofluids in thermal devices.

Chein and Huang [22]observed the functional behaviour of electronic compounds when using nanofluids and found a greater cooling effect. Nassan et al. [23] carried out an experimentally study on the contribution of Al_2O_3/water and CuO/water nanofluids to the enhancement of heat transfer in a square cross-section cupric duct under the constant heat flux condition. They suggested the CuO/water nanofluid results higher convective heat transfer coefficient in comparison to Al_2O_3/water nanofluid. Rostamani et al. [24] experimentally studied the turbulent flow condition of alumina (Al_2O_3), copper oxide (CuO), and titanium oxide (TiO_2) nanofluids with different volume concentrations flowing through a two-dimensional duct. They observed that the heat transfer rate of nanofluids depends on the particles volume concentrations.

Heris et al. [25]carried out an experimental study on convective heat transfer through circular tube under laminar flow and constant wall temperature boundary condition. The results showed that the heat transfer coefficient of CuO and Al_2O_3, nanofluids enhances with increasing nanoparticles concentrations as well as by increasing the Peclet number. Similarly, Heris et al. [26]also investigated the heat transfer characteristics of turbine oil-based CuO, TiO_2, and, Al_2O_3 nanofluids in a circular tube. They suggested that the highest Nusselt number ratios at 0.50 % volume concentration of TiO_2/turbine oil, Al_2O_3/turbine oil nanofluids and the Reynolds number value of 800 are 1.38, 1.31, and 1.15, respectively. They found that the performance index of all the nanofluids under consideration is more than one. Finally, they concluded that the turbine oil base nanofluids results more heat transfer.

Khan et al. [27] investigated the energy efficiencies of solar parabolic dish system for power generation with the nanofluids such as Al_2O_3, CuO and TiO_2.. They reported that the Al_2O_3oil based nanofluid gives 33.73% overall energy and 36.27%, exergy efficiencies. They interpreted that this is 0.27% higher than the TiO2/oil nanofluid and 0.91% higher than CuO/oil based nanofluid. They also reported the receiver's tube convective heat transfer coefficient is improved by adding more amount of nanoparticles. Al-Rashed et al. [28] investigated the cooling effect of central processing unit using nanofluids by both experimentally and numerically.

Siddiquiet al. [29] examined the role of Al_2O_3 and Cu nanofluids at the 0.251% and 0.11% volume concentrations in a flat plate heat sink used to cool the microprocessor. They studied that the Al_2O_3/water nanofluid gives greater heat transfer rate than the Cu/water nanofluid at low Reynolds number. However, the Cu/water nanofluids results more effectively at high Reynolds number. Ali et al. [30]reported the ZnO/-water nanofluids at the volumetric concentrations of 0.01%, 0.08%, 0.2% and 0.3% enhances the heat transfer performance of a car radiator. They found that the considerable increase in heat transfer because of the use of ZnO/water nanofluids when compared with the base fluids.

Similarly, Ali et al. [31] applied the MgO/nanofluids in a car radiator to analyse the thermal performances at different flow rates and various volumetric concentrations. They observed that the 0.12% volume concentration nanofluids offers 31% heat transfer enhancement when compared with water. They also examined the effect of increasing the temperature of nanofluids by 8 °C gives 6% heat transfer enhancement. They further reported that the stability of nanofluids is the challenge for applying nanofluids.

Arshad et al. [32] studied the thermal and hydrodynamic performance of distilled water and graphene nanoplatelets (GNPs) nanofluid in an integral fin heat sink. They presented that the nanofluids results in desirable thermal performances than the water. Ali et al. [33] experimentally studied the effect of pin fin angle of heat sink channel on convective heat transfer coefficient and thermal resistance with graphene nanoplatelets (GNPs)/water nanofluids as coolant at the flow rate range of 0.25–0.75 L per minute. They found the thermal reductions are 22.17%, 18.28% and 14.60% for 22.5°, 45° and 90° heat sink angles respectively.

Ghasemi et al. [34] investigated the heat dissipation behaviours of electronic cooling devices with different shapes by using CuO/water nanofluids and with the Computational Fluid Dynamics (CFD) simulations. Similarly, Ghasemi et al. [35] observed the thermal performance of electronic cooling devices with different heat transfer surface. They concluded that the thermal resistance of the heat sink decreases when the volume fraction of nanoparticles is increased. Jajja et al. [36]investigated the base temperature of micro channel heat sink by using multi walled carbon nanotube nanofluid and by varying the fin spacing of (0.2 mm, 0.5 mm, 1.0 mm, and 1.5 mm). They found that the reduction of spacing of and using nanofluids fin improves the heat transfer coefficient up to 15% and the thermal resistance reduces.

Raisi et al. [37]numerically investigated the heat flow characteristics of the microchannel by using Cu–water based nanofluids. They found that the heat transfer coefficient is considerably changed with the change in particle volume concentrcation at the maximum Reynolds number. Prasher and Chang [38] studied experimentally the effect of reducing channel widths above a hotspot with a heat flux of 1250 W/cm^2. Their results demonstrated that a lower thermal resistance is achieved by narrowing the channel above the hotspot.

Ghasemi et al. [39]observed that the heat transfer coefficient increases with an increase in volume concentration of nanoparticles and suggested that this is due to addition of more numbers of nanoparticles in the nanofluid which yields to an increase in thermal conductivity than the water. Kumar et al. [40] observed the random movement of nanoparticles contributes to the enhanced heat transfer coefficient. They also observed that the friction factor increases over particle volume concentration and this is due to increased nanofluid viscosity while increasing particle volume concentration.

Heris et al. [41]experimentally investigated the inclination angle of the cavity in the order of angles 0°, 45° and 90° with respect to the horizontal position. They employed the three Al_2O_3, TiO_2, and CuO

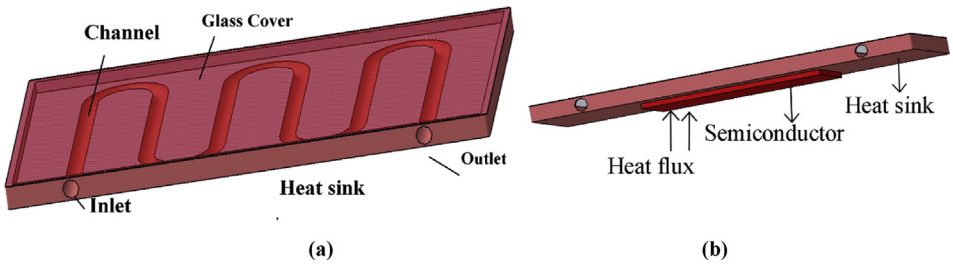

Fig. 1. Schemmatic Diagram of channel heat sink with semiconductor, (a) top view, (b) side view.

turbine oil (TO) based nanofluids at the weight concentration of 0.2%, 0.5%, and 0.8%. They found that TiO_2/water nanofluids at 0.8% and at 90° inclination gives the maximum Nusselt number. In addition, Heris et al. [42]reported the effect of applying an electric field on the performance of a two-phase flow closed thermosiphon handling CuO/water nanofluid and the evaporator section filled with 40% of target fluid. They found that and applying an electric field on nanofluid increases the thermal efficiency up to 30% as compared with pure water.

Sheikholeslami [43] studied the role of magnetic field on CuO–H_2O nanofluid flow inside a porous channel and simulated the flow by means of Lattice Boltzmann method. The results demonstrated that convective mode progresses with increase of Darcy number (*Da*) and Reynolds number (*Re)*. Sheikholeslami [44] also investigated that CuO nanoparticles with various shapes of nanoparticles into the base fluid to augment conduction mode. The results demonstrated that the maximum rate of solidification can be obtained for Platelet shape nanoparticles. Mehrjou et al. [45]experimentally analysed the convective heat transfer of CuO/water nanofluid in a square cross-section duct under turbulent flow condition. They noticed that the heat transfer coefficient and Nusselt number are improved by increasing the nanoparticles concentrations and the Peclet number. They also reported that the heat transfer rates in the triangle, square, and rectangle shape is smaller than the circular tubes.

In addition, Arshad et al. [46]experimentally investigated the heat transfer and pressure drop characteristic associated with minichannel heat sink. They found that pressure drop increases with the decrease of heating power and this is significant for TiO_2nanofluid as compared to distilled water due to viscosity variation with temperature. Heris et al. [47]numerically examined the laminar flow-forced convective heat transfer of Al_2O_3/water nanofluid in a triangular duct under constant wall temperature condition. They reported that the numerical solutions show that the Nusselt number increases by increasing decreasing the size of the nanoparticles at a fixed concentration and increasing the nanoparticles concentration by fixing the size of the nanoparticles.

It is clear from the literature that, little work has been done on the cooler heatsink with a channel by using CuO/water nanofluid to dissipate heat. In this paper, heat transfer analysis on channel heat sink with CuO/water nanofluids is carried out numerically with the objectives of using CuO/water nanofluid as coolant on heat transfer coefficient, Nusselt number, reliability, and power consumption of semiconductor.

2. Methodology

2.1. Mathematical modelling

2.1.1. Description

The schematic diagram of heatsink with the channel is shown in Fig. 1. The heat sinks are designed with a channel to extract more heat from the semiconductor surface. The channel heatsink has an inlet and outlet with a hydraulic diameter of 0.0022m.The length of the single channel is 30mm, inlet and outlet diameter of a channel are 2.5mm, while the total dimensions of the heatsink are 50 mm × 75 mm with a wall thickness of 1.5mm. The channel is filled with CuO-water nanofluid having nanoparticles volume concentration of 0.25, 0.5 and 0.75% as coolant. The bottom wall of the heatsink is getting heated by a uniform generation of heat flux 60W/cm^2.

Table 1
Thermo-physical properties of water and CuO nanoparticle [34].

Properties	Distilled water	CuO nanoparticle
Density ρ(kg/m^3)	997.1	6500
Specific heat C_p(J/kg.K)	4179	540
Thermal conductivity k (W/m.K)	0.613	18
Dynamic Viscosity μ(N.s/m^2)	0.001003	–
Mean diameter (nm)		29

2.1.2. Boundary conditions

The boundary conditions are given, as contributions for the model, in ANSYS – CFD simulation. The flow of fluid depends on laminar and the analogous boundary conditions for the channel heat sink are given below. The coolant is utilized in this numerical calculation through the inlet is water, and CuO/water nanofluid and its relating thermo-physical properties are revealed in Table 1.

In this analysis, the coolant under consideration is taken as single phase medium, the entry temperature of coolant is 20 °C and the temperatures are maintained constant to achieve the equilibrium conditions.

2.1.3. Numerical analysis

The modelling of channel heat sink is done and meshed by using CFD software ANSYS Fluent v12. The type of the element is Aluminium. The total number of elements and nodes for a channel heatsink is 278989 and 70181 respectively. The accuracy of the CFD is yielded by enhancing mesh quality. Fig. 2 shows the meshing of channel heatsink bottom view, top view, and the channel of heat sink using ANSYS computational software.

The SIMPLE (Semi-Implicit Method for Pressure-Linked Equation) algorithm has been used to solve the momentum equations in terms of velocity and pressure. In this numerical investigation, CuO/water nanofluid is used as the coolant in the channel heat sink.

The governing mass, momentum, and energy Eqs. (1), (2), (3), (4), and (5) are written as follows for the incompressible, laminar and steady-state fluid flow [35, 48]:

Continuity equation:

$$\frac{\partial u}{\partial x}+\frac{\partial v}{\partial y}+\frac{\partial w}{\partial z}=0 \tag{1}$$

Momentum equation [22]:

$$\rho_f\left(u\frac{\partial u}{\partial x}+v\frac{\partial u}{\partial y}+w\frac{\partial u}{\partial z}\right)=-\frac{\partial \rho}{\partial x}+\mu_f\left(\frac{\partial^2 u}{\partial x^2}+\frac{\partial^2 u}{\partial y^2}+\frac{\partial^2 u}{\partial z^2}\right) \tag{2}$$

$$\rho_f\left(u\frac{\partial v}{\partial x}+v\frac{\partial v}{\partial y}+w\frac{\partial v}{\partial z}\right)=-\frac{\partial \rho}{\partial y}+\mu_f\left(\frac{\partial^2 v}{\partial x^2}+\frac{\partial^2 v}{\partial y^2}+\frac{\partial^2 v}{\partial z^2}\right) \tag{3}$$

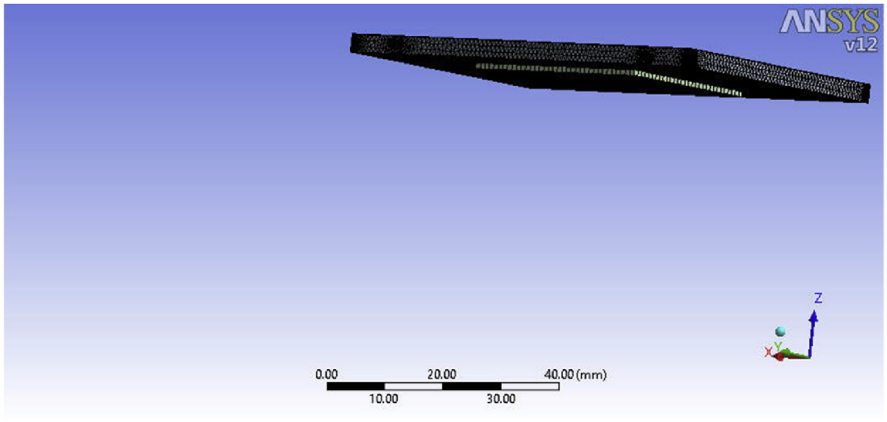

(a)

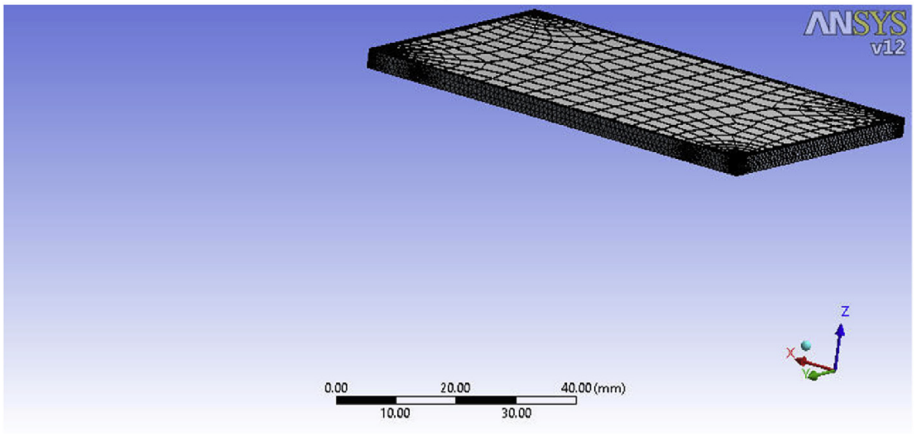

(b)

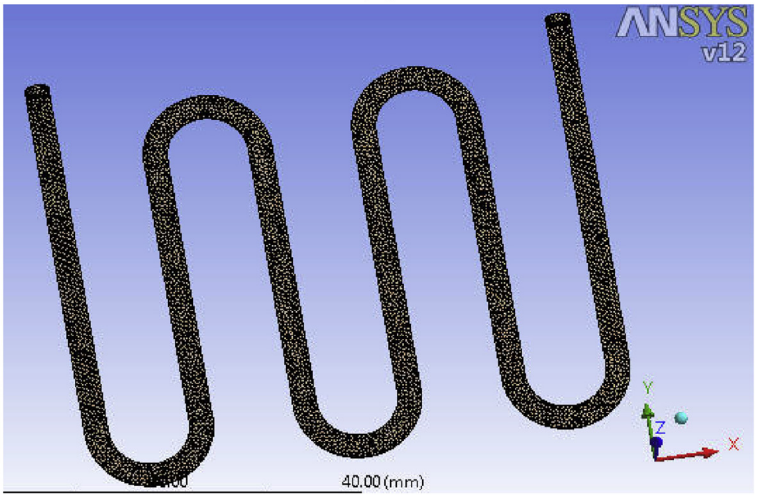

(c)

Fig. 2. Computational meshes for a channel heatsink, (a) bottom view, (b) top view, (c) channel.

$$\rho_f\left(u\frac{\partial w}{\partial x}+v\frac{\partial w}{\partial y}+w\frac{\partial w}{\partial z}\right)=-\frac{\partial \rho}{\partial z}+\mu_f\left(\frac{\partial^2 w}{\partial x^2}+\frac{\partial^2 w}{\partial y^2}+\frac{\partial^2 w}{\partial z^2}\right) \quad (4)$$

Where ρ_f is the density and μ_f is the dynamic viscosity of the nanofluids and p is the pressure of the coolant.

Energy equation for nanofluids [35]:

$$\rho_f C_{pf}\left(u\frac{\partial T_f}{\partial x}+v\frac{\partial T_f}{\partial y}+w\frac{\partial T_f}{\partial z}\right)=K_f\left(\frac{\partial^2 T_f}{\partial x^2}+\frac{\partial^2 T_f}{\partial y^2}+\frac{\partial^2 T_f}{\partial z^2}\right) \quad (5)$$

Where T_f is the temperature of the coolant, $C_{p,f}$ is the specific heat, and K_f is thermal conductivity of distilled water.

The calculation for Reynolds number (*Re*), heat transfer coefficient, Nusselt number, friction factor and thermal resistance is given by Eqs. (6), (7), (8), (9), (10), (11), and (12)

Reynolds number (*Re*)is calculated based on the hydraulic diameter and volume fractions of nanoparticles for channel heatsink respectively [49].

Reynolds number is defined as:

$$Re=\rho U_m D_h/\mu \quad (6)$$

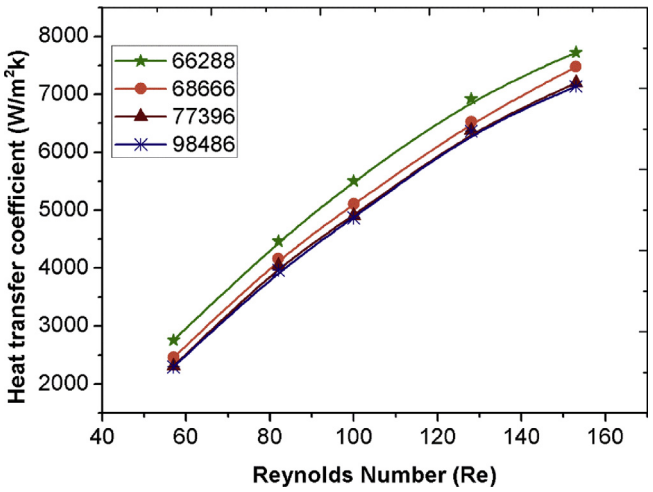

Fig. 3. Grid independence test analysis.

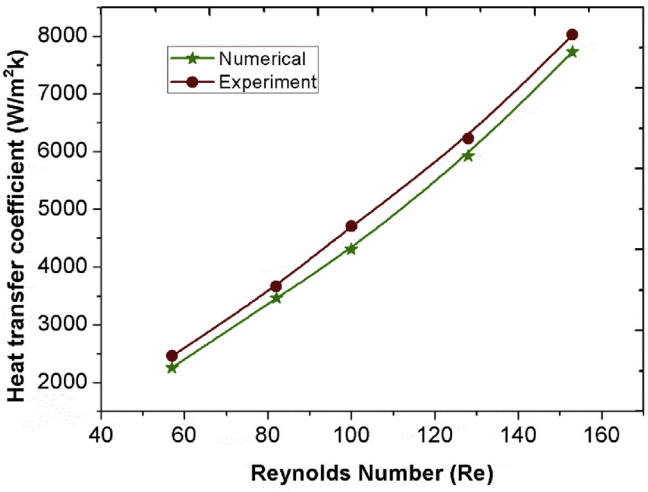

Fig. 4. Comparison of numerical results with experimental data.

Heat transfer rate is calculated by

$$Q = m_w Cp_w (T_{wout} - T_{win}) \tag{7}$$

The average heat transfer coefficient h_{ave}:

$$h_{ave} = \frac{Q}{A_h \Delta T_m} \tag{8}$$

The average Nusselt number is defined as [50]:

$$Nu = \frac{h_{ave} D_h}{k} \tag{9}$$

The friction factor through the heatsink is defined as [50]

$$f = \frac{2D_h \Delta p}{\rho u^2 L} \tag{10}$$

The thermal resistance of the channel heatsink is calculated by

$$R_{th} = \frac{T_{\max} - T_{\min}}{q} \tag{11}$$

Where T_{max} and T_{min} are the maximum and minimum temperatures observed in the channel heatsink respectively.

Pumping power PP is directly proportional to the mass flow rate and pressure drop and is found from Eq. (12).

$$PP = \Delta p Q \tag{12}$$

Similarly the thermos-physical properties of the nanofluid such as thermal conductivity (k_{eff}), density (ρ_{eff}), heat capacity ($C_{p,eff}$), and dynamic viscosity (μ_{eff}) are calculated using the proposed correlations which are defined as following Eqs. (13), (14), (15), and (16) [50]:

Density [50]:

$$\rho_{eff} = (1-\varphi)\rho_f + \varphi\rho_p \tag{13}$$

Heat capacity [50]:

$$C_{p,eff} = \frac{(1-\varphi)(\rho C_{p,f})_f + \varphi(\rho C_p)_p}{\rho_{nf}} \tag{14}$$

Effective dynamic viscosity [50]:

$$\mu_{eff} = \frac{\mu_f}{(1-\varphi)^{2.5}} \tag{15}$$

Thermal conductivity [50]:

$$k_{eff} = \frac{k_p + (n-1)k_f - (n-1)\varphi(k_f - k_p)}{k_p + (n-1)k_f + \varphi(k_f - k_p)} k_f \tag{16}$$

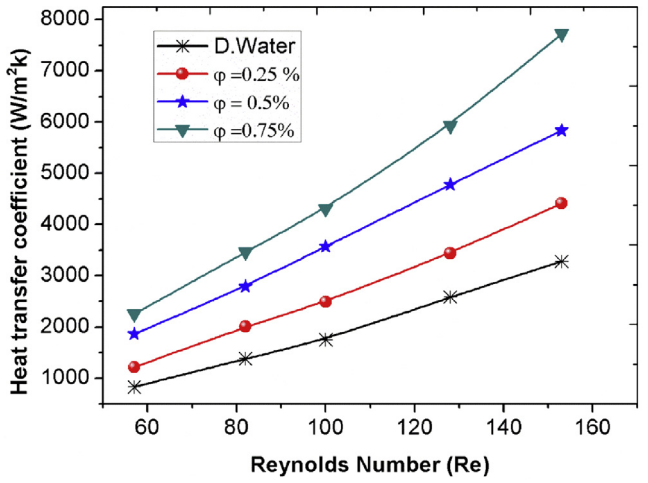

Fig. 5. Variation of Heat transfer coefficient with Reynolds number.

Where K_p, K_f and k_{efff} are thermal conductivity of nanoparticles, base fluid and nanofluid respectively. Also, n is the empirical shape factor. For spherical nanoparticles, the empirical shape factor is 3 (n = 3).

2.2. Grid independence test

In this work, four grids have been generated for the channel heat sink to investigate the grid independence and validate the precision of numerical solutions. The four nodes such as 66288, 68666, 77396, and 98486 which are used to calculate the heat transfer coefficient with respect to Reynolds number. The obtained results shows that there is a very small difference between the grid with nodes 77396 and others. Therefore, in this study the grid with nodes 77396 has been used to achieve the results. Fig. 3, shows the results of grid independence test.

3. Results and discussion

The channel heat sink model with a coolant such as water and CuO/water nanofluids is analyzed by CFD simulations. The results are obtained for the three different volume concentrations such as φ = 0.25%, φ = 0.5% and φ = 0.75%. The heat transfer coefficient, Reynolds number, Nusselt number, thermal resistance, friction factor, power consumption and reliability for a given volume fractions of nanoparticles are discussed and compared the results with water.

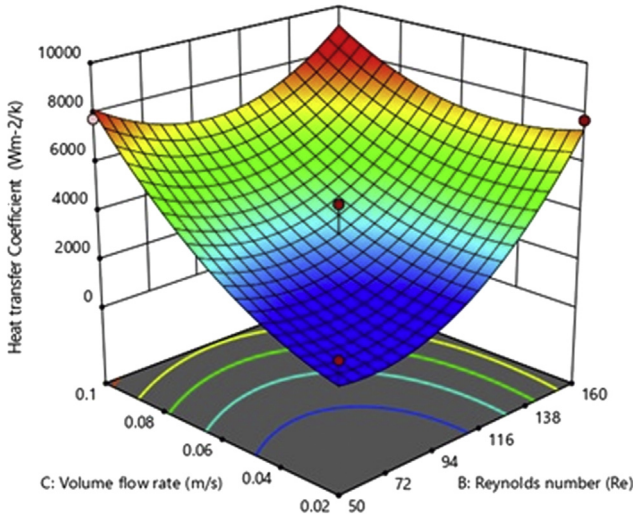

Fig. 6. 3D graph of heat transfer coefficient.

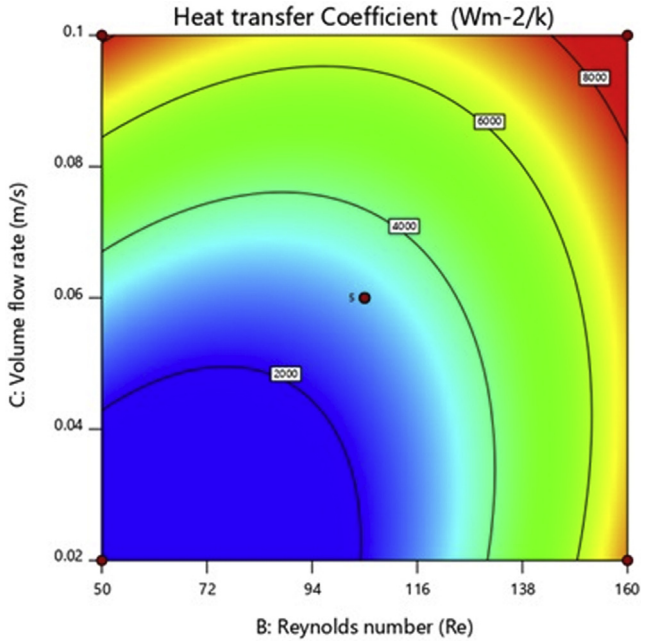

Fig. 7. Contour diagram of heat transfer coefficient.

3.1. Validate analysis

The numerical calculation results are validated with the experimental data as shown in Fig. 4. The data for heat transfer coefficient of the sink under consideration is is 2% deviation from the experimental data. The variation of the heat transfer coefficient with respect to the function of different volume flow rate for a hydraulic diameter of channels is shown in Fig. 5.

The graph shows that the average heat transfer coefficient increases with respect to Reynolds number. Kumar et al. [51] numerically examined the cooling performance of an electronic chip with different fin thickness and length by using ANSYS –Fluent (v12). The results revealed that the heat transfer rate of water is 9.5%, and 1.4% greater than air and engine oil at the same Reynolds number.

It is observed that the heat transfer characteristic of the channel heatsink is improved by an increase of inlet velocity. It is found that the heat transfer coefficient of $\varphi = 0.25\%$, $\varphi = 0.5\%$, $\varphi = 0.75\%$ CuO/water

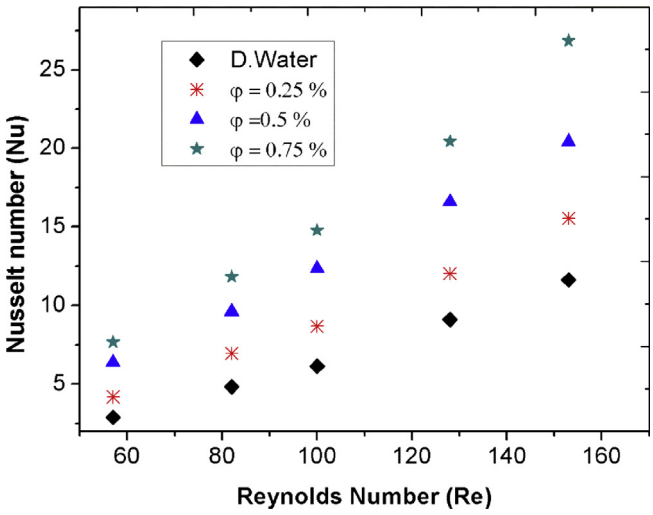

Fig. 8. Variations of Nusselt number with Reynolds number.

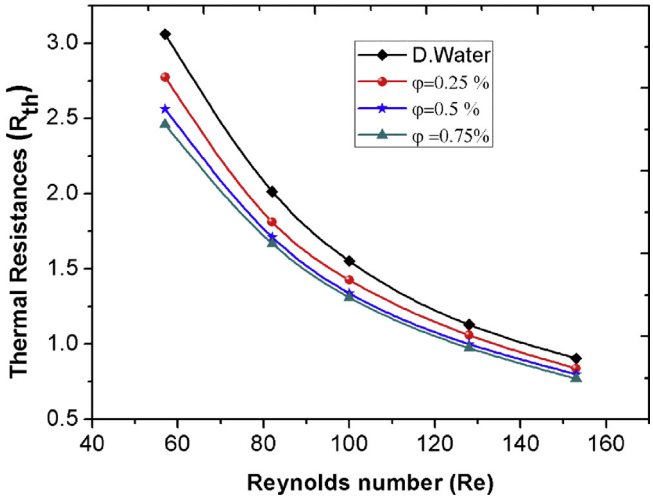

Fig. 9. Thermal resistance versus Reynolds number.

nanofluids are 25%, 43% and 57% higher than the water respectively. The improved heat transfer coefficient is due to the higher thermal conductivity of nanofluids and the presence of more nanoparticles in the base fluids. Here, the maximum heat transfer coefficient is occur at 0.75% nanofluids.

Fig. 6 is obtained from design expert 11 software, it shows the 3D graph effects of heat transfer coefficients with respect to volume flow rate and Reynolds number. Similarly, Fig. 7, the contour diagram of heat transfer coefficients to show the maximum and minimum value. Heris et al. [52]numerically investigated the convective heat transfer of Al_2O_3/water, CuO/water and Cu/water nanofluids in a square cross-section duct. The results revealed that the Nusselt number is enhanced by increasing the concentration and decreasing the size of nanoparticles. The enhancement of Nusselt number is 77%, 68% and 59% for Cu/water, CuO/water and Al_2O_3/water nanofluids respectively at 4.0% volume concentration and at the size of 10nm.

Fig. 8 shows the variations of Nusselt number as a function of Reynolds number with different volume concentration of CuO/water nanofluids in the channel heatsink. It is found that use of CuO/water nanofluids in the channel heatsink improves the heat transfer characteristics. This graph also shows that by increasing the volume concentrations (0.25%, 0.5%, and 0.75%) of nanofluids the Nusselt number increases. It is examined that higher the Reynolds number, higher the

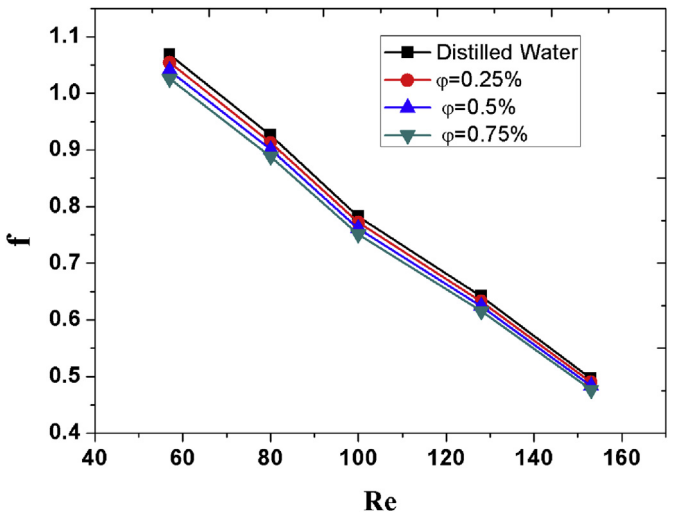

Fig. 10. Variation of friction factor versus Reynolds number.

Nusselt number (Nu) and the Nusselt number are found to be 25 %, 43 %, and 56% higher than water for 0.25%, 0.5%, and 0.75% of CuO/water nanofluids respectively. This is because of more convective heat transfer current.

The important factor utilized in semiconductor heat dissipation is the thermal conduction which the reverse of thermal resistance to study the overall heat transfer performance. The thermal resistance measurement is the indication of input power give to the channel. Fig. 9, presents the relationship between the Reynolds number and the thermal resistance with the volume concentrations of 0.25%, 0.5%, and 0.75% of CuO/water nanofluids. From this figure, it can be interpreted that higher Reynolds number has a lower thermal resistance in the channel heatsink. The reason for decreasing the thermal resistance is due to the higher velocity when Re is higher. This higher fluid velocity reduces the thermal resistance between been the fluid particles with the MWCNTs and higher concentration nanofluids has more thermal conductivity. This results the more thermal transportation and this is inversely interrelated to the convective thermal resistance.

It is observed that the higher volume concentrations of CuO/water nanofluids have lower thermal resistance than water. In addition, the thermal resistance of the channel heatsink using CuO/water nanofluid with a nanoparticle volume concentrations of (0.25%, 0.5%, and 0.75%) is increased from 6% to 13% as compared to that of using water. As shown in Fig. 10, the friction factor of nanofluid in the channel heatsink decreases with increasing Reynolds number. This is because the friction factor and velocity have an inverse relationship, therefore, the friction factor reduces by increasing the Reynolds number. It is observed that φ = 0.25% nanofluid has lower friction factor than φ = 0.5% and φ = 0.75%. This is due to the presence of less solid nanoparticle in the water.

Heris et al. [53] investigated the pressure drop and performance characteristics of Al_2O_3/water and CuO/water nanofluids in a triangular duct under constant heat flux and laminar flow. They proposed the pressure drop increases by 35% with an increase of volume fraction of nanoparticles in comparison with the base fluid.

The inlet velocity of water flows in the channel heat sink is shown in Fig. 11. The volume flow rate of inlet water and nanofluids is 0.02 m/s to 1 m/s. It is evident that the temperature of the fluid at the exit of the channel is decreased by increasing the inlet velocity. It is clear from Fig. 12 that the wall temperature reduces significantly by using the coolant. It is observed that the highest heat transfer rates are identified for each concentration at the highest Re.

3.2. Cooling versus power dissipation

The one of the most important factors in VLSI design circuits is the power dissipation. It is because of power consumption, reliability, and process speed are highly interconnected. Power dissipation is calculated by equation [17]

$$T_j = T_a + R_{th(j-a)} * P \tag{17}$$

Where T_a is the ambient temperature, T_j is the junction temperature, $R_{th(j-a)}$ is thermal resistance between junction and ambient temperature and P is power dissipation. It is well known that the chip power consumption and temperature are circular dependence between them. However, the fact that electronic chip may reach thermal runaway condition at extreme temperature.

Fig. 13, shows the relationship between power dissipation and temperature in the channel heatsink. The graph shows that the power dissipation of a semiconductor is decreased when the coolant is used. It is found that the power dissipation are 3%, 6%, and 8% lower than water for 0.25%, 0.5%, and 0.75% of CuO/water nanofluids respectively.

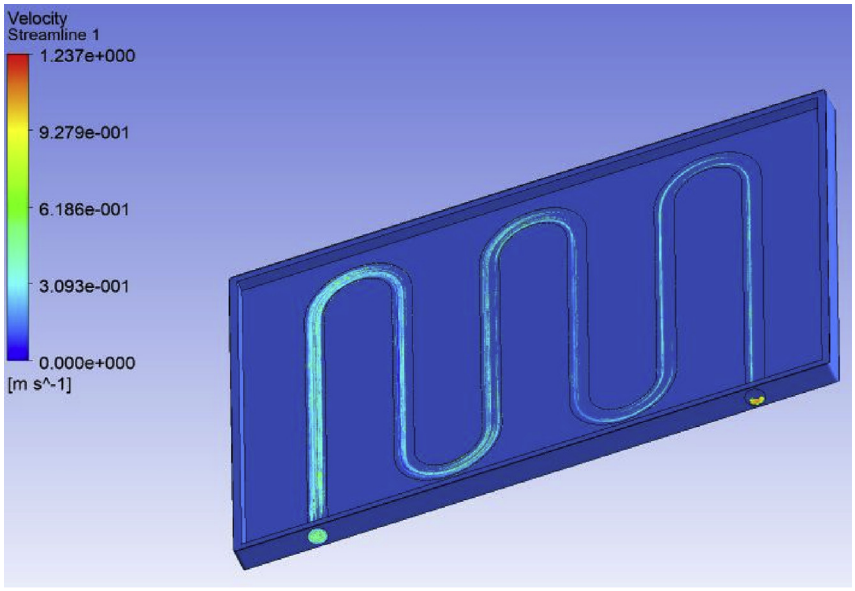

Fig. 11. Inlet velocity flow of water in the heatsink.

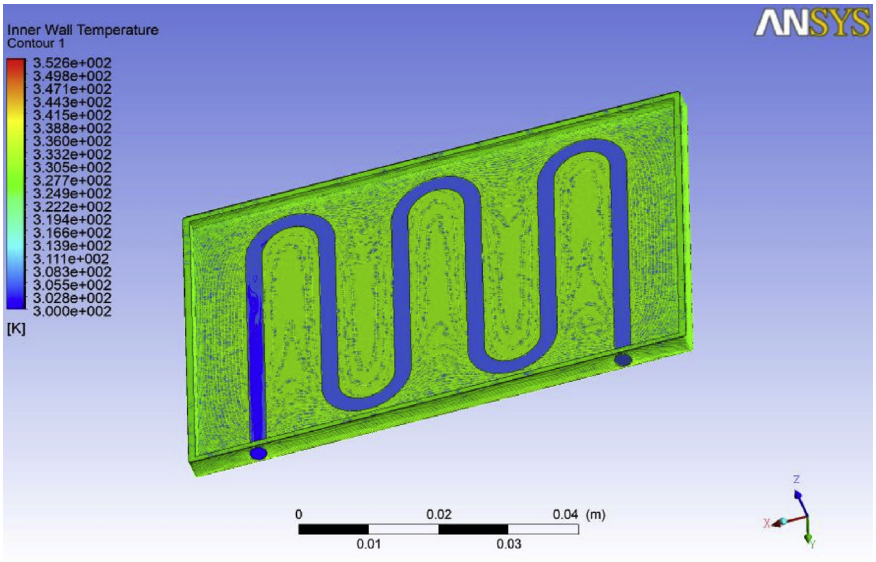

Fig. 12. Change of Wall temperature using coolant.

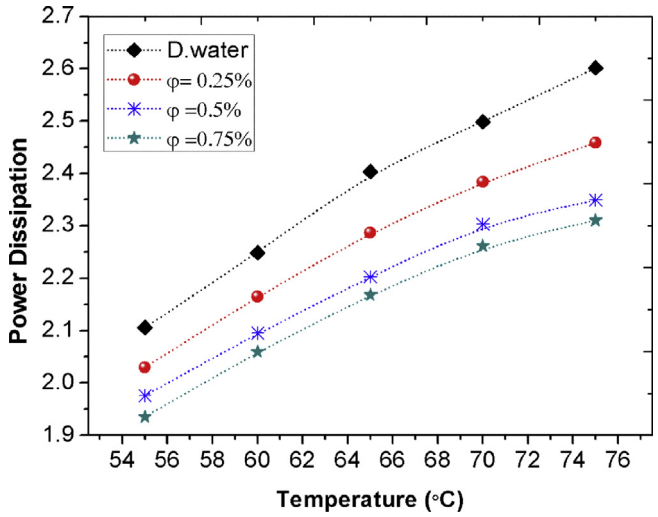

Fig. 13. Power dissipation of heat sink with respect to temperature.

Fig. 14, shows the contour diagram of power dissipation with respect to thermal resistance and ambient temperature. Power consumption is reduced when the thermal resistance is decreased. It leads to the reliability of semiconductor when coolant is used in the channel sink.

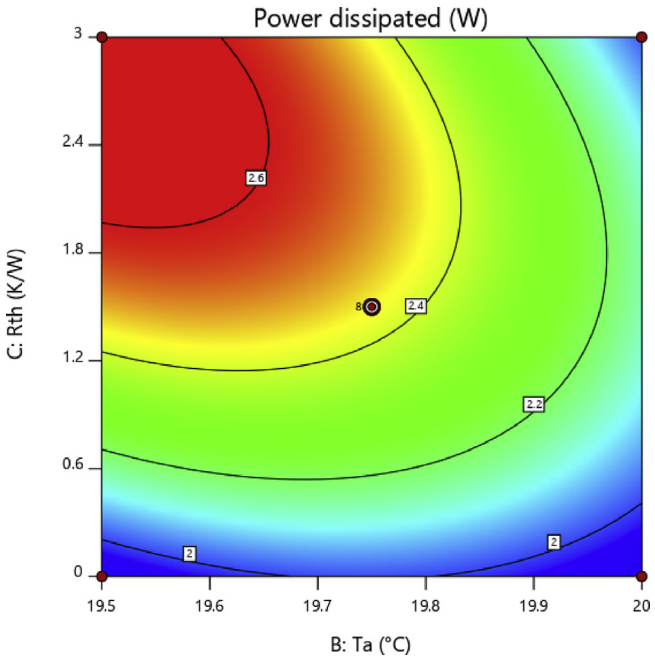

Fig. 14. Contour diagram of Power dissipation of heatsink.

3.3. Cooling versus reliability

The reliability of semiconductor is based on the calculation of the failure rate [54]. The failure of a semiconductor is mostly associated with overheating and subsequent burning. Reliability of semiconductor is designed by considering the temperature. Some of the failure mechanism that affect the life time of the semiconductors are oxide defects, corrosion, and photoresist and charge injection. The failure rate, Acceleration Factor, failures in time, MTTF (Mean Time to Failure) for reliability calculation is given by Eqs. (18), (19), (20), (21), and (22). Failure Rate (λ) in this model is calculated by dividing the total number of failures or rejection by the cumulative time of operation [54].

$$EDH = D^{*}H^{*}A_f \tag{18}$$

Where

D = Number of Devices Tested
H = Test Hours per Device
A_f = Acceleration Factor resultant from the Arrhenius equation

The Failure Rate (λ) per hour is shown by [54]:

$$\lambda_{hour} = \frac{r}{D^{*}H^{*}A_f} = \frac{r}{EDH} \tag{19}$$

Where: r = number of failures or rejects.

The Acceleration Factor (A_f) is derived from the Arrhenius equation and given by [54]:

$$A_f = e^{E_a/k}\left({}^{1}/_{T_{use}} - {}^{1}/_{T_{test}}\right) \tag{20}$$

Where

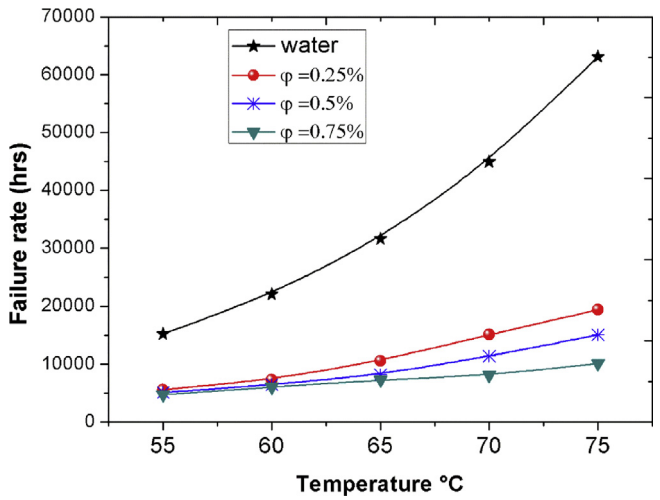

Fig. 15. Failure rate versus temperature.

E_a = Activation Energy (eV) of the different failure mode.
K (Boltzmann's Constant) = 8.617×10^{-5}eV/°K.
T_{use} = Use Temperature (standardized in°K)
T_{test} = Test Temperature (HTOL temperature in °K)
eV = electron volts.

FIT (Failures in Time) is a typical diligence value defined as the Failure Rate (λ) per billion hours.

$$FIT = \lambda_{FIT} = \lambda_{hours} * 10^9 \quad (21)$$

MTTF (Mean Time to Failure) is given by [54]:

$$MTTF_{hours} = {}^1/_{\lambda_{hours}} \text{ or } MTTF_{years} = {}^1/_{(\lambda_{hours} * 24 * 365)} \quad (22)$$

Fig. 15, shows the variation of failure rate of the semiconductor versus temperature in the channel heatsink. The graph shows that the reliability of a semiconductor using CuO/water nanofluids is improved. It is found that the failure rate is 69%, 76%, and 84% for 0.25%, 0.5%, 0.75% of CuO/water nanofluids in channel heat sink and failure rate is smaller than water. The higher reliability of semiconductor using CuO/water nanofluids is simply because of effective cooling of the semiconductor with more thermal conductivity CuO nanofluids.

4. Conclusions

In this research work, the thermal performance of a semiconductor using channel heat sink is investigated numerically with a different volume fraction of nanofluids such as φ = 0.25%, φ = 0.5%, φ = 0.75% of CuO/water nanofluids and water by using ANSYS–Fluent (v12). It is observed that higher the Reynolds number, higher the Nusselt number (Nu) and found to be 25%, 43%, and 56% higher than water. It is found that the thermal resistance and friction factor decrease when increasing nanoparticle concentration and with Reynolds number. This is may be due to higher thermal conductivity of CuO/water nanofluids and the random movement of nanoparticles. Also studied that the heat transfer coefficient increases by 25%, 43% and 57% for 0.25%, 0.5%, and 0.75% of CuO/water nanofluids respectively than the water. The reason for this improvement is due to less thermal resistance and effective mixing of nanoparticles in the base fluids which carries more heat. The power dissipation of an electronic chip with channel heat sink is decreased up to 8.09% when using volume fraction (φ = 0.75%) of CuO/water nanofluids than the water and deteriorate of failure rate of semiconductor by 69%, 76%, and 84%. The contribution to the reliability improvement is that there is no sudden change in temperature which leads to give the reduced thermal stress when nanofluids are supplied.

Declarations

Author contribution statement

C.M. Arun Kumar & P.C. Mukeshkumar: Conceived and designed the experiments; Performed the experiments; Analyzed and interpreted the data; Contributed reagents, materials, analysis tools or data; Wrote the paper.

Funding statement

This research did not receive any specific grant from funding agencies in the public, commercial, or not-for-profit sectors.

Competing interest statement

The authors declare no conflict of interest.

Additional information

No additional information is available for this paper.

References

[1] D.B. Tuckerman, R.F.W. Pease, High-performance heat sinking for VLSI, IEEE Electron. Device Lett. (1981).
[2] X. Wei, Y. Joshi, Optimization study of stacked micro-channel heat sinks for micro-electronic cooling. InterSociety Conference on Thermal and Thermomechanical Phenomena in Electronic Systems, ITHERM, 2002.
[3] K. Nishino, M. Samada, K. Kasuya, K. Torii, Turbulence statistics in the stagnation region of an axisymmetric impinging jet flow, Int. J. Heat Fluid Flow (1996).
[4] Y.M. Chung, K.H. Luo, Unsteady heat transfer analysis of an impinging jet, J. Heat Transf. (2002).
[5] Z. Zhao, C.T. Avedisian, Enhancing forced air convection heat transfer from an array of parallel plate fins using a heat pipe, Int. J. Heat Mass Transf. (1997).
[6] Y. Wang, K. Vafai, An experimental investigation of the thermal performance of an asymmetrical flat plate heat pipe, Int. J. Heat Mass Transf. (2000).
[7] K.S. Kim, M.H. Won, J.W. Kim, B.J. Back, Heat pipe cooling technology for desktop PC CPU, Appl. Therm. Eng. (2003).
[8] S.A. Jajja, W. Ali, H.M. Ali, A.M. Ali, Water cooled minichannel heat sinks for microprocessor cooling: effect of fin spacing, Appl. Therm. Eng. (2014).
[9] K. Toh, X. Chen, J. Chai, Numerical computation of fluid flow and heat transfer in microchannels, Int. J. Heat Mass Transf. (2002).
[10] I. Tiselj, G. Hetsroni, B. Mavko, A. Mosyak, E. Pogrebnyak, Z. Segal, Effect of axial conduction on the heat transfer in micro-channels, Int. J. Heat Mass Transf. (2004).
[11] X.L. Xie, W.Q. Tao, Y.L. He, Numerical study of turbulent heat transfer and pressure drop characteristics in a water-cooled minichannel heat sink, J. Electron. Packaging Trans. ASME (2007).
[12] X.L. Xie, Z.J. Liu, Y.L. He, W.Q. Tao, Numerical study of laminar heat transfer and pressure drop characteristics in a water-cooled minichannel heat sink, Appl. Therm. Eng. (2009).
[13] P. Cova, N. Delmonte, F. Giuliani, M. Citterio, S. Latorre, M. Lazzaroni, A. Lanza, Thermal optimization of water heat sink for power converters with tight thermal constraints, Microelectron. Reliab. (2013).
[14] M. Conrad, A. Diatlov, R.W. De Doncker, Purpose, potential and realization of chip-attached micro-pin fin heat sinks, Microelectron. Reliab. (2015).
[15] S.U.S. Choi, J.A. Eastman, Enhancing thermal conductivity of fluids with nanoparticles, ASME Int. Mech. Eng. Cong. Expos. (1995).
[16] S. Lee, S.U.-S. Choi, S. Li, J.A. Eastman, Measuring thermal conductivity of fluids containing oxide nanoparticles, J. Heat Transf. (1999).
[17] B.X. Wang, L.P. Zhou, X.F. Peng, A fractal model for predicting the effective thermal conductivity of liquid with suspension of nanoparticles, Int. J. Heat Mass Transf. (2003).
[18] J. Koo, C. Kleinstreuer, A new thermal conductivity model for nanofluids, J. Nanoparticle Res. (2004).
[19] M.U. Sajid, H.M. Ali, Thermal conductivity of hybrid nanofluids: a critical review, Int. J. Heat Mass Transf. (2018).
[20] H.M. Ali, H. Babar, T.R. Shah, M.U. Sajid, M.A. Qasim, S. Javed, H.M. Ali, H. Babar, T.R. Shah, M.U. Sajid, M.A. Qasim, S. Javed, Preparation techniques of TiO2 nanofluids and challenges: a review, Appl. Sci. (2018).
[21] M.U. Sajid, H.M. Ali, Recent advances in application of nanofluids in heat transfer devices: a critical review, Renew. Sustain. Energy Rev. (2019).
[22] R. Chein, G. Huang, Analysis of microchannel heat sink performance using nanofluids, Appl. Therm. Eng. (2005).
[23] T.H. Nassan, S.Z. Heris, S.H. Noie, A comparison of experimental heat transfer characteristics for Al 2 O 3/water and CuO/water nanofluids in square cross-section duct, Int. Commun. Heat Mass Transf. (2010).

[24] M. Rostamani, S.F. Hosseinizadeh, M. Gorji, J.M. Khodadadi, Numerical study of turbulent forced convection flow of nanofluids in a long horizontal duct considering variable properties, Int. Commun. Heat Mass Transf. (2010).
[25] S.Z. Heris, S.G. Etemad, M.N. Esfahany, Experimental investigation of oxide nanofluids laminar flow convective heat transfer, Int. Commun. Heat Mass Transf. (2006).
[26] S.Z. Heris, F. Farzin, H. Sardarabadi, Experimental comparison among thermal characteristics of three metal oxide nanoparticles/turbine oil-based nanofluids under laminar flow regime, Int. J. Thermophys. (2015).
[27] M.S. Khan, M. Abid, H.M. Ali, K.P. Amber, M.A. Bashir, S. Javed, Comparative performance assessment of solar dish assisted s-CO2 Brayton cycle using nanofluids, Appl. Therm. Eng. (2019).
[28] M.H. Al-Rashed, G. Dzido, M. Korpyś, J. Smołka, J. Wójcik, Investigation on the CPU nanofluid cooling, Microelectron. Reliab. (2016).
[29] A.M. Siddiqui, W. Arshad, H.M. Ali, M. Ali, M.A. Nasir, Evaluation of nanofluids performance for simulated microprocessor, Therm. Sci. (2017).
[30] H.M. Ali, H. Ali, H. Liaquat, H.T. Bin Maqsood, M.A. Nadir, Experimental investigation of convective heat transfer augmentation for car radiator using ZnO-water nanofluids, Energy (2015).
[31] H.M. Ali, M.D. Azhar, M. Saleem, Q.S. Saeed, A. Saieed, Heat transfer enhancement of car radiator using aqua based magnesium oxide nanofluids, Therm. Sci. (2015).
[32] W. Arshad, H.M. Ali, Graphene nanoplatelets nanofluids thermal and hydrodynamic performance on integral fin heat sink, Int. J. Heat Mass Transf. (2017).
[33] H.M. Ali, W. Arshad, Effect of channel angle of pin-fin heat sink on heat transfer performance using water based graphene nanoplatelets nanofluids, Int. J. Heat Mass Transf. (2017).
[34] S.E. Ghasemi, A.A. Ranjbar, M.J. Hosseini, Numerical study on effect of CuO-water nanofluid on cooling performance of two different cross-sectional heat sinks, Adv. Powder Technol. (2017).
[35] S.E. Ghasemi, A.A. Ranjbar, M.J. Hosseini, Experimental and numerical investigation of circular minichannel heat sinks with various hydraulic diameter for electronic cooling application, Microelectron. Reliab. (2017).
[36] S.A. Jajja, W. Ali, H.M. Ali, Multiwalled carbon nanotube nanofluid for thermal management of high heat generating computer processor, Heat Transf. Asian Res. (2014).
[37] A. Raisi, B. Ghasemi, S.M. Aminossadati, A numerical study on the forced convection of laminar nanofluid in a microchannel with both slip and no-slip conditions, Numer. Heat Transf. Part A: Applications (2011).
[38] R. Prasher, J.-Y. Chang, Cooling of Electronic Chips Using Microchannel and Micro-pin Fin Heat Exchangers, 2009.
[39] S.E. Ghasemi, A.A. Ranjbar, M.J. Hosseini, Forced convective heat transfer of nanofluid as a coolant flowing through a heat sink: experimental and numerical study, J. Mol. Liq. (2017).
[40] P.C. Mukesh Kumar, J. Kumar, S. Suresh, Experimental investigation on convective heat transfer and friction factor in a helically coiled tube with Al2O3/water nanofluid, J. Mech. Sci. Technol. (2013).
[41] S.Z. Heris, M.B. Pour, O. Mahian, S. Wongwises, A comparative experimental study on the natural convection heat transfer of different metal oxide nanopowders suspended in turbine oil inside an inclined cavity, Int. J. Heat Mass Transf. (2014).
[42] S.Z. Heris, F. Mohammadpur, O. Mahian, A.Z. Sahin, Experimental study of two phase closed thermosyphon using cuo/water nanofluid in the presence of electric field, Exp. Heat Transf. (2015).
[43] M. Sheikholeslami, Numerical investigation for CuO-H2O nanofluid flow in a porous channel with magnetic field using mesoscopic method, J. Mol. Liq. (2018).
[44] M. Sheikholeslami, Finite element method for PCM solidification in existence of CuO nanoparticles, J. Mol. Liq. (2018).
[45] B. Mehrjou, S. Zeinali Heris, K. Mohamadifard, Experimental study of CuO/water nanofluid turbulent convective heat transfer in square cross-section duct, Exp. Heat Transf. (2015).
[46] W. Arshad, H.M. Ali, Experimental investigation of heat transfer and pressure drop in a straight minichannel heat sink using TiO2nanofluid, Int. J. Heat Mass Transf. (2017).
[47] S.Z. Heris, S.H. Noie, E. Talaii, J. Sargolzaei, Numerical investigation of al 2 o 3/ water nanofluid laminar convective heat transfer through triangular ducts, Nanoscale Res. Lett. (2011).
[48] S. Patankar, Numerical Heat Transfer and Fluid Flow, 1980.
[49] A.A.Y. Al-Waaly, M.C. Paul, P. Dobson, Liquid cooling of non-uniform heat flux of a chip circuit by subchannels, Appl. Therm. Eng. (2017).
[50] S.E. Ghasemi, A.A. Ranjbar, M.J. Hosseini, Experimental evaluation of cooling performance of circular heat sinks for heat dissipation from electronic chips using nanofluid, Mech. Res. Commun. (2017).
[51] P.C.M. Kumar, C.M.A. kumar, Influence of aspect ratio on thermal performance of heat sink using ansys, J. Appl. Fluid Mech. 11 (2018) 45–52. Special Issue.
[52] S.Z. Heris, A. Kazemi-Beydokhti, S.H. Noie, S. Rezvan, Numerical study on convective heat transfer of AL 2 O 3/water, CuO/water and Cu/water nanofluids through square cross-section duct in laminar flow, Eng. Appl. Comput. Fluid Mech. (2012).
[53] S.Z. Heris, F. Ahmadi, O. Mahian, Pressure drop and performance characteristics of water-based Al 2 O 3 and CuO nanofluids in a triangular duct, J. Dispersion Sci. Technol. (2013).
[54] Microsemi, Calculating Reliability Using FIT & MTTF: Arrhenius HTOL Model, Rev, 2012.